Removal of Phase Artifacts From fMRI Data Using a Stockwell Transform Filter Improves Brain Activity Detection

Bradley G. Goodyear,* Hongmei Zhu, Robert A. Brown, and J. Ross Mitchell

A novel and automated technique is described for removing fMRI image artifacts resulting from motion outside of the imaging field of view. The technique is based on the Stockwell transform (ST), a mathematical operation that provides the frequency content at each time point within a time-varying signal. Using this technique, 1D Fourier transforms (FTs) are performed on raw image data to obtain phase profiles. The time series of phase magnitude for each and every point in the phase profile is then subjected to the ST to obtain a time-frequency spectrum. The temporal location of an artifact is identified based on the magnitude of a frequency component relative to the median magnitude of that frequency's occurrence over all time points. After each artifact frequency is removed by replacing its magnitude with the median magnitude, an inverse ST is applied to regain the MR signal. Brain activity detection within fMRI datasets is improved by significantly reducing image artifacts that overlap anatomical regions of interest. The major advantage of ST-filtering is that artifact frequencies may be removed within a narrow time-window, while preserving the frequency information at all other time points. Magn Reson Med 51:16–21, 2004. © 2003 Wiley-Liss, Inc.

Key words: fMRI; artifacts; filtering; Stockwell transform; Fourier transform; motion

Movement occurring outside of the imaging field of view (FOV) can lead to MR phase variations during image collection giving rise to magnitude artifacts in reconstructed images. Gradient-recalled echo, echo planar imaging (GRE-EPI), commonly used in functional MRI (fMRI) applications, is especially susceptible to this phenomenon since image data collection is relatively slow in the phase-encode direction. As a result, ghosting artifacts occur in the phase-encode direction of an EPI image that may overlap anatomical regions of interest (ROIs). The removal of these artifacts is of particular importance in fMRI since analysis techniques rely on the variation of image pixel intensity over time to identify brain regions involved in a specified task (for review, see Ref. 1). This has placed major limitations on many fMRI studies. For example, studies involving language have relied on the mental generation of words (2–4) rather than speech production due to the phase artifacts that accompany jaw movements and the resonating oral cavity (5,6). Attempts to study speech by designing postprocessing strategies to remove motion-related artifacts have been successful (7); however, magnitude artifacts arising from the variation of phase due to motion outside of the imaging field of view are not correctable using existing motion correction techniques since rigid motion of the brain is not the result of the artifact. In this case, false-positive or false-negative brain activity may occur.

One common technique to correct for variations in phase is to use a navigator echo correction scheme (8). The navigator echo (i.e., a nonphase encoded echo collected after each RF pulse) is used to register the phase of image raw data to the phase of the first collected image. This has proven useful for the removal of phase variations due to physiological fluctuations such as respiration. However, if other phase variations occur during the collection of an image, such as that resulting from sudden motion outside of the imaging FOV, artifacts will remain since the navigator echo will not characterize these additional phase changes. Hence, an additional phase correction scheme is required.

One common approach to remove additional artifacts is to apply a temporal filter to image pixel intensity after images have been reconstructed (9,10) using a 1D Fourier transform (FT) to determine the average magnitude of frequency components within the time series of pixel intensity. Filtering of artifact frequencies is usually achieved by multiplying the resulting frequency spectrum by a bandpass filter (e.g., a Hamming window) that is unity near frequencies that are to be maintained and zero at artifact frequencies (for review, see Ref. 11). The major limitation of this technique is that the filter is applied indiscriminately to all time points of the series. This may be of concern if the frequency content of the signal is important, such as determining accurate relative timing measurements or when significant brain activity is based on the magnitude of the paradigm frequency relative to all other frequencies. A short time-window FT (STFT) can be used to obtain the temporal location of frequency components; however, a priori knowledge of the frequency content of the signal is required to set the window size. This may be further addressed using the Wavelet transform (12,13), which has been used successfully in fMRI (14). However, the output of Wavelet transform analysis can be difficult to interpret.

A technique that may help address these issues is one that employs the Stockwell transform (ST) (15,16), a mathematical operation closely resembling the Fourier trans-

Departments of Radiology and Clinical Neurosciences, Seaman Family MR Research Centre, University of Calgary and Foothills Medical Centre, Calgary, Alberta T2N 2T9, Canada.

Grant sponsors: Alberta Heritage Foundation for Medical Research, Canadian Institutes for Health Research, Multiple Sclerosis Society of Canada.

*Correspondence to: Bradley Goodyear, PhD, Seaman Family MR Research Centre, Foothills Medical Centre, 1403 29th Street NW, Calgary, AB Canada T2N 2T9. E-mail: goodyear@ucalgary.ca

Received 24 March 2003; revised 30 July 2003; accepted 15 September 2003.

DOI 10.1002/mrm.10681
Published online in Wiley InterScience (www.interscience.wiley.com).

form. The ST of a 1D signal in time, f(t), is a 2D function in time, t, and frequency, ν, namely:

$$S(\tau,\nu) \equiv S\{f(t)\} = \int_{-\infty}^{+\infty} f(t) w_s\left(\frac{t-\tau}{1/\nu}\right) \exp(-2\pi i t \nu) dt$$

$$= FT\{f(t) \cdot w_s((t-\tau),\nu)\}. \quad [1]$$

Note the similarity to the Fourier transform, except the ST analyzes the signal using localized frequency-dependent Gaussian time windows, w_S, of the form:

$$w_s((t-\tau),\nu) = \frac{|\nu|}{\sqrt{2\pi}} \exp\left(-\frac{(t-\tau)^2\nu^2}{2}\right). \quad [2]$$

As a result, narrower windows are used at higher frequencies and wider windows are used at lower frequencies. The ST can therefore be considered a short-time Fourier transform with a multiscaled localizing time window (for further discussion, see Ref. 17).

Recently, the ST has been introduced as a tool for MRI analysis (17) and for filtering pixel time courses in fMRI (18). In this study, the ST is introduced as a tool for filtering residual high-frequency phase artifacts unsuccessfully removed by navigator echo from fMRI data prior to image reconstruction. In addition, as a demonstration of the superiority of the ST over commonly used low-pass filtering techniques, ST filtering and low-pass FT filtering were applied to a computer-generated dataset of time courses simulating the hemodynamic response to visual stimulation with high-frequency artifacts introduced at selected time points.

MATERIALS AND METHODS

The ST filtering technique was written in the C programming language and consists of the following steps. A time-varying signal is subjected to the ST to obtain a 2D spectrum of frequency component magnitude as a function of time. The median magnitude of each frequency component over time is calculated and frequency artifact locations are labeled in time when magnitude exceeds three times the median (Although arbitrary, it has been our experience that three times the median is a good indicator of frequency artifact). Artifact frequencies do not occur discretely, but rather are "blotches" or "smears" in the ST spectrum (i.e., they occur over a narrow range of both time and frequency). Hence, artifact regions are taken to extend from the artifact location (i.e., where magnitude exceeds three times the median) to where the magnitude falls below the median magnitude. This successfully encompasses the artifact. The magnitudes within these regions are replaced with the median magnitude of a frequency's occurrence. To regain the time-varying signal, the magnitude of each frequency is summed over all time indices to collapse the spectrum to a 1D function and an inverse FT is applied.

Simulation Study

To compare the ST filter to low-pass filtering, 529 time courses of 220 points were synthesized to simulate seven repetitions of a hemodynamic response to 6 sec of stimulation occurring at 30-sec intervals. A model of the hemodynamic response to this stimulus was derived from the convolution of the boxcar stimulus presentation time course (i.e., seven presentations of 6 sec ON, 24 sec OFF) with an ideal hemodynamic response function (HRF) for a 1-sec stimulus (19). Zero-mean Gaussian noise was added to simulate real responses. Each time course was then subjected to a correlation analysis with the modeled HRF, and the correlation coefficient, r, for each time course calculated. This provided a distribution of expected r values for the simulated data. High-frequency artifacts were added at two chosen time intervals. ST filtering was then compared to low-pass filtering (using four times the paradigm frequency as the high-frequency cutoff (11)) in the ability to remove the artifacts and regain the expected distribution of r values when correlated again with the modeled HRF. ST filtering was repeated for a dataset free of the high-frequency noise to ensure that the ST filter did not alter time courses free of artifact.

Human Studies

All fMRI experiments were performed using a 3 T MR imaging system (General Electric, Waukesha, WI) equipped with a quadrature birdcage RF head coil. Six healthy volunteers gave written informed consent prior to participating. T_2^*-weighted images of ten 4-mm thick oblique-axial slices parallel to the calcarine sulcus were collected using a GRE-EPI sequence (TE = 30 ms, TR = 1000 ms, two interleaved segments, 22 cm FOV, 96 × 96 matrix). A navigator echo was collected for each segment to correct for phase fluctuations due to respiration (14). The phase-encode direction was chosen to be anterior–posterior such that image ghosts, if present, would overlap with visual cortex. Subjects wore liquid crystal display goggles (Resonance Technology, Northridge, CA) connected to the video output of a personal computer. A 6 Hz black-white contrast-reversing checkerboard pattern was presented for 6 sec (*activation phase*), immediately followed by 24 sec of a static gray screen (*rest phase*). This was repeated seven times during one experimental run. During additional experiments, each subject was asked to 1) take two deep breaths, 2) cough lightly, or 3) talk briefly (say "mi-mi-mi") when the checkerboard appeared for a second time during an experimental run and when the checkerboard disappeared for a fourth time during an experimental run. This potentially introduced phase artifacts at two separate time points within the hemodynamic response. Image data were zero-padded to 128 × 128 before reconstruction.

Since artifacts were introduced in the raw data phase, the ST-filtering technique was applied in the following manner. After navigator echo correction, a 1D FT was applied to the raw data along each frequency-encoded echo and the phase, p, of each complex pair (R, I) of the FT-transformed data was calculated to create a phase profile. This was repeated for all time points (i.e., image

volumes). The time course of each and every point within a phase profile was then subjected to the ST filter as described above. Once a time course of the filtered phase, p', was regained, new real and imaginary values (R', I') of the complex data were calculated according to:

$$R' = R\cos(p' - p) - I\sin(p' - p) \quad [3]$$

$$I' = R\sin(p' - p) + I\cos(p' - p) \quad [4]$$

The resulting phase profiles were subjected to an inverse 1D FT to regain the raw image data, which were then reconstructed as images. Maps of activity in response to the checkerboard stimulus were created for each experimental run (i.e., deep breathing, coughing, talking, normal) with and without ST filtering by identifying image pixels exhibiting a significant correlation ($r > 0.4$, $P < 0.01$) with the modeled HRF. The amount of activation (i.e., number of map pixels multiplied by each pixel's strength of correlation, r) was then recorded.

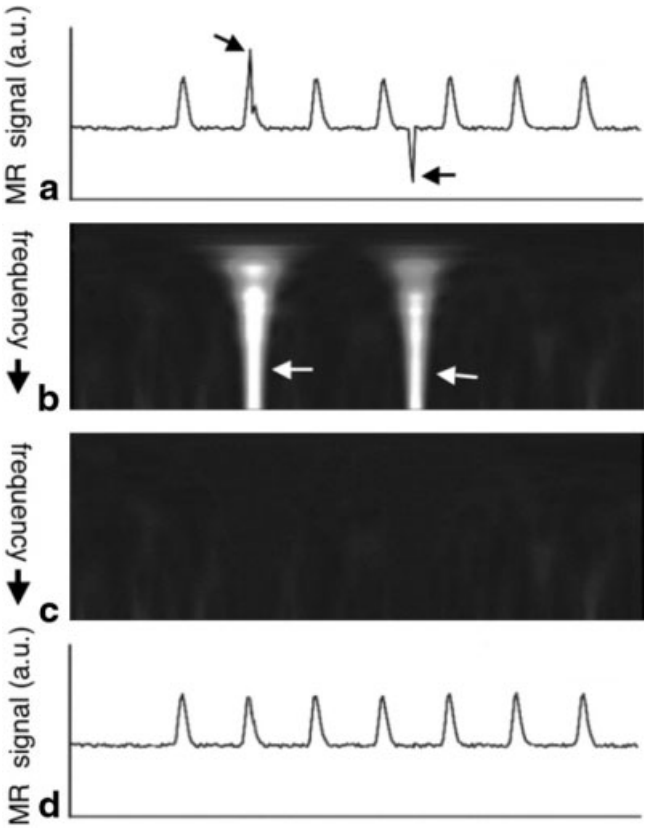

FIG. 1. Stockwell transform (ST) filtering of simulated fMRI time courses. **a:** High-frequency artifacts were inserted at two time-points (as indicated by arrows) into time courses simulating image pixel intensity. **b:** The Stockwell frequency/time spectrum for the time-varying signal in **a**. The hot areas in the spectrum (white) indicate the presence of high-frequency artifacts in the time-varying signal. **c:** Artifacts are filtered from the spectrum by replacing the magnitude of the artifact frequency within these white areas with the median of the frequency's occurrence over time. **d:** The time course of simulated image pixel intensity after ST filtering obtaining by summing each frequency component over all time indices and performing a 1D inverse FT.

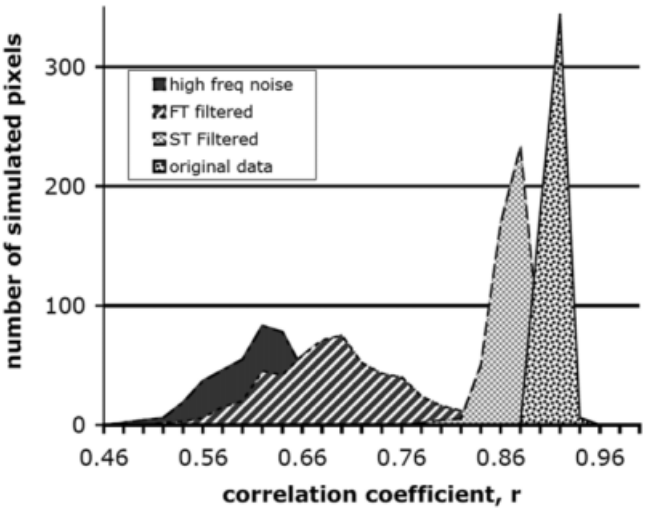

FIG. 2. A comparison of ST-filtering and high-pass filtering of fMRI time courses. Histograms showing pixel cross-correlation coefficients, r, resulting from cross-correlation of each simulated pixel's intensity time course with a modeled hemodynamic response function. Five hundred twenty-nine time courses were generated in this simulation study. The distribution at the far right is for 529 time courses before the addition of high-frequency noise and represents an artifact-free distribution. Other distributions are shown for 529 time courses after high-frequency noise was added, after low-pass FT-filtering of high-frequency artifacts, and after Stockwell transform (ST)-filtering of the high-frequency artifacts.

RESULTS

Figure 1 demonstrates ST filtering of a pixel time course. Figure 1a is one of the 529 simulated image pixel time courses with high-frequency artifacts introduced at two selected time points. Figure 1b is its time-frequency ST spectrum. High-frequency artifacts are easily identified within the ST spectrum. The filtering of these artifacts from the ST spectrum is demonstrated in Fig. 1c, where artifact magnitude have been replaced with the median magnitude. The regained filtered time course is shown in Fig. 1d. The high-frequency artifacts are removed and the frequency content of the remaining signal is preserved. It is important to note that ST-filtering did not alter artifact-free simulated time courses (not shown).

The results of the cross-correlation analysis of the 529 simulated time courses are shown in Fig. 2. As expected, the cross-correlation coefficient of each simulated pixel's time course decreased after introducing high-frequency noise. Low-pass FT filtering did increase cross-correlation coefficients; however, this method indiscriminately removed high frequencies from the entire time course and shifted the cross-correlation distribution to larger values. Filtering using the ST removed artifact frequencies only at artifact locations and maintained the frequency content of the signal elsewhere; the cross-correlation increased significantly and the distribution regained the shape of the original artifact-free distribution.

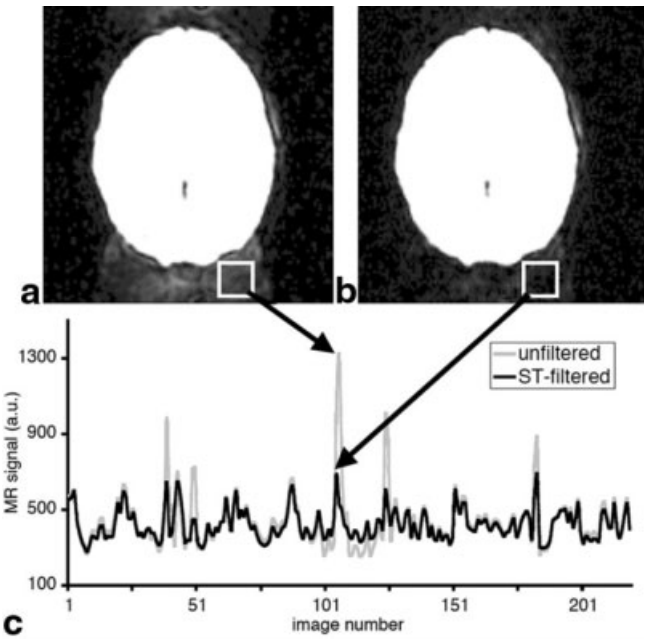

FIG. 3. Stockwell transform (ST) filtering of fMRI data significantly reduces ghost intensity. **a:** T_2*-weighted image collected when a subject was coughing. Ghost intensity is relatively high and overlaps the visual cortex. **b:** ST filtering reduces ghost intensity magnitude to the near baseline levels. **c:** Average time course of image intensity for image pixels inside the white boxes. ST filtering removes high-frequency artifacts from the MR signal.

Figure 3 shows a representative image of one slice from one subject when a high-frequency artifact occurred due to the subject coughing. The intensity of image ghosts is relatively high (Fig. 3a) and potentially masks the hemodynamic response. ST-filtering of high-frequency artifacts from raw data phase reduced the intensity of ghosts to near baseline levels (Fig. 3b), as well as at points where unmonitored artifacts occurred. More important, the ST filter greatly reduced pixel intensity fluctuations in anatomical ROIs. This is apparent from Figs. 4 and 5, which show fMRI maps in visual cortex (Fig. 4a, without ST filtering; Fig. 4b, with ST filtering) and intensity time courses of single map pixels. Differences between the maps in Fig. 4a,b are apparent. Several map pixels were removed by ST filtering, while others were added. Figure 5 shows time courses of two single map pixels. The pixel of Fig. 5a was not in the map for the unfiltered data. After ST filtering, this pixel was determined to be significantly correlated with the visual stimulation. The pixel of Fig. 5b was a false-positive map pixel that was subsequently removed from the map after ST filtering. For the six subjects in this study and for all conditions, there was a significant effect of the ST filter in terms of the amount of activation detected (Table 1).

DISCUSSION

Navigator echo correction is successful at removing phase fluctuations due to physiological processes such as respiration. The ST filter, on the other hand, does not perform well nor is it designed to alter phase oscillations at such low frequencies. The ST filter is designed to remove high-frequency phase artifacts associated with motion outside of the imaging FOV. The experiments in this study were designed to demonstrate that navigator echo correction alone is not sufficient when motion occurs outside of the imaging FOV. The ST filter in addition to the navigator

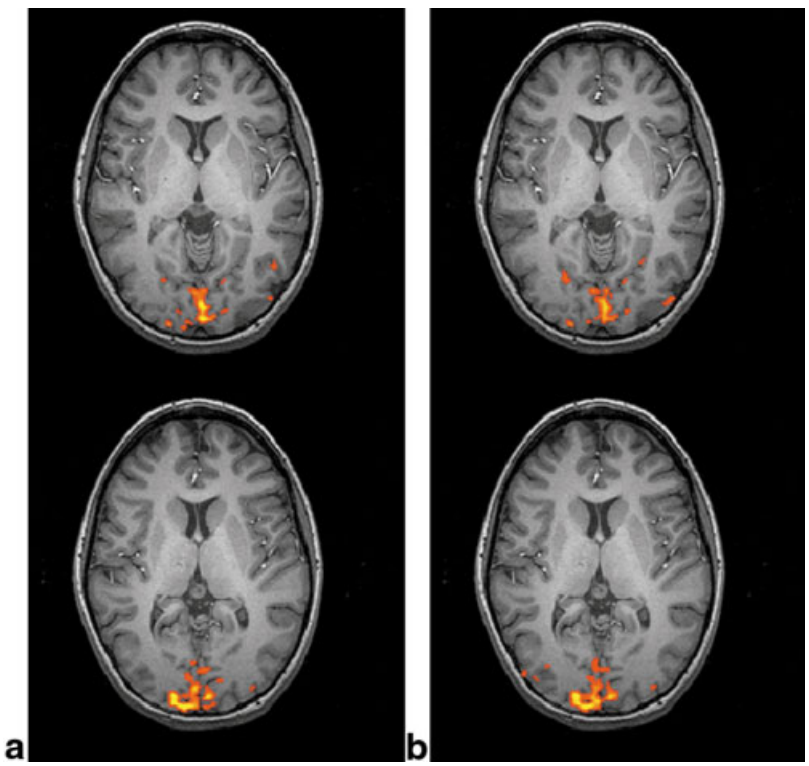

FIG. 4. fMRI maps and time courses of activity in the visual cortex of one subject in response to the checkerboard stimulus. **a:** Map created before ST filtering. **b:** Map created after ST filtering. Each map consists of image pixels exhibiting a correlation with a modeled hemodynamic response function ($r > 0.4$, $P < 0.01$).

echo is a powerful combination for the removal of phase artifacts prior to image construction.

The ST filter is applicable only to regions of the image where SNR is relatively high, that is, inside the object. In these regions the ratio of phase magnitude to noise is also high and frequency content over time is discernible. In low SNR regions, phase magnitude is essentially random and high-frequency artifacts are masked and do not contribute appreciably to image artifacts after reconstruction.

The ST filter does not always increase or decrease map pixel significance. On average in this study, pixels in maps created before filtering did exhibit a reduction in correlation with the expected HRF as a result of ST-filtering because the high-frequency artifact was manifested as a relatively large increase in MR signal superimposed on the hemodynamic response. The ST filter is especially useful for image pixels that are near statistical threshold, as it reduces both false-positive and false-negative map pixels by reducing large high-frequency signal superimposed on the hemodynamic response and by reducing signal variance. It is also important, however, to remove artifacts from strongly correlated pixels, especially if analyses are to be extended to calculate the strength of the fMRI response within map pixels.

It is interesting to note that the ST filter also significantly changed maps for "normal" experimental runs when the subject was not asked to purposefully introduce noise. All of our subjects were MR-naïve, and at times may have changed breathing patterns, coughed, and/or cleared throats, potentially introducing MR phase artifacts. Nonetheless, the ST filter was successful at identifying and removing these artifacts as well. This demonstrates the true effectiveness of the ST filter, as artifacts of this nature are unpredictable and are not usually monitored. It is anticipated that ST filtering will prove especially useful in patient fMRI studies, as patients are more prone to introduce artifacts due to their discomfort or restlessness.

A novel, automated, and intuitive technique for filtering unpredictable high-frequency phase variations from fMRI datasets occurring as a result of motion outside of the imaging FOV based on the ST has been introduced. This technique may offer the possibility of exploring cortical processes with overt speech components as well as swallowing. As well, this technique may prove useful for improving datasets collected while objects or subjects' hands and arms are moved near the head, such as in reaching or pointing experiments.

Table 1
ST filtering significantly alters the amount of activation detected in the cortex

Condition	Significance of ST filter in altering the amount of detected activation, p
Breathe	0.015
Cough	0.049
Talk	0.040
Normal	0.036

For each condition and across subjects, the amount of activation (calculated as the number of pixels times the strength of correlation of each pixel with expected HRF) was significantly different after ST-filtering ($p < 0.05$, six subjects).

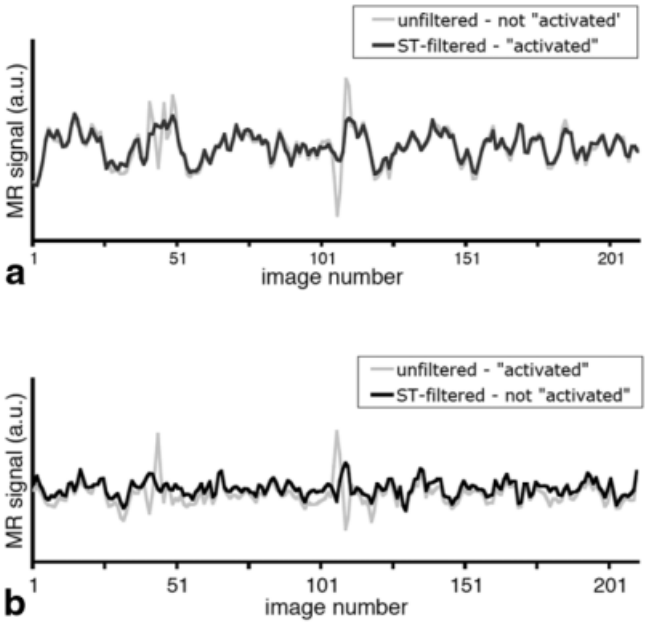

FIG. 5. **a:** Time course of a single map pixel from this panel that is not present in **b**. ST-filtering increased the correlation to above statistical threshold (i.e., ST-filtering decreases false-negatives). **b:** Time course of a single map pixel from this panel that is not present in **a**. ST-filtering decreased the correlation to below statistical threshold (ST-filtering decreases false-positives).

ACKNOWLEDGMENT

The authors thank Dr. Louis Lauzon for technical assistance and helpful discussions.

REFERENCES

1. Smith SM. Overview of fMRI analysis. In: Jezzard P, Matthews PM, Smith SM, editors. Functional MRI: an introduction to methods. Oxford: Oxford University Press; 2001. p 215–228.
2. McGraw P, Mathews VP, Wang Y, Phillips MD. Approach to functional magnetic resonance imaging of language based on models of language organization. Neuroimag Clin N Am 2001;11:343–353.
3. Martin RC. Language processing: functional organization and neuroanatomical basis. Annu Rev Psychol 2003;54:55–59.
4. Small SL, Burton MW. Functional magnetic resonance imaging studies of language. Curr Neurol Neurosci Rep 2002;2:505–510.
5. Yetkin FZ, Haughton VM, Cox RW, Hyde J, Birn RM, Wong EC, Prost R. Effect of motion outside the field of view on functional MR. AJNR Am J Neuroradiol 1996;17:1005–1009.
6. Birn RM, Bandettini PA, Cox RW, Shaker R. Event-related fMRI of tasks involving brief motion. Hum Brain Mapp 1999;7:106–114.
7. Huang J, Carr TH, Cao Y. Comparing cortical activations for silent and overt speech using event-related fMRI. Hum Brain Mapp 2002;15:39–53.
8. Hu X, Kim SG. Reduction of signal fluctuation in functional MRI using navigator echoes. Magn Reson Med 1994;31:495–503.
9. Glover GH, Li TQ, Ress D. Image-based method for retrospective correction of physiological motion effects in fMRI: RETROICOR. Magn Reson Med 2000;44:162–167.
10. Chuang KH, Chen JH. IMPACT: image-based physiological artifacts estimation and correction technique for functional MRI. Magn Reson Med 2001;46:344–353.

11. Smith SM. Preparing fMRI data for statistical analysis. In: Jezzard P, Matthews PM, Smith SM, editors. Functional MRI: an introduction to methods. Oxford: Oxford University Press; 2001. p 229–241.
12. von Tscharner V, Thulborn KR. Specified-resolution wavelet analysis of activation patterns from BOLD contrast fMRI. Hum Brain Mapp 1998;6:378–382.
13. Brammer MJ. Multidimensional wavelet analysis of functional magnetic resonance images. Magn Reson Med 2001;46:344–353.
14. LaConte SM, Ngan SC, Hu X. Wavelet transform-based Wiener filtering of event-related fMRI data. Magn Reson Med 2000;44:746–757.
15. Stockwell RG, Mansinha L, Lowe RP. Localization of the complex spectrum: the S transform. IEEE Trans Signal Proc 1996;44:998–1001.
16. Mansinha L, Stockwell RG, Lowe RP, Eramian M, Schincariol RA. Local S-spectrum analysis of 1-D and 2-D data. Phys Earth Plan Inter 1997;103:329–336.
17. Zhu H, Goodyear BG, Lauzon ML, Brown RA, Mayer G, Law AG, Mansinha L, Mitchell JR. A new local multiscale Fourier analysis for MRI. Med Physics 2003;30:1134–1141.
18. Goodyear BG, Zhu H, Frayne R, Mitchell JR. Filtering noise from fMRI data using the Stockwell transform. In: Proc 10th Annual Meeting ISMRM, Honolulu, 2000. p 1419.
19. Birn RM, Cox RW, Bandettini PA. Detection versus estimation in event-related fMRI: choosing the optimal stimulus timing. Neuroimage 2002; 15:252–264.